(4)

AFGL-TR-88-0199

DOWNWARD CONTINUATION OF THE FREE-AIR GRAVITY ANOMALIES TO THE ELLIPSOID USING THE GRADIENT SOLUTION, POISSON'S INTEGRAL AND TERRAIN CORRECTION-NUMERICAL COMPARISON AND COMPUTATIONS.

Yan Ming Wang

DEPARTMENT OF GEODETIC SCIENCE AND SURVEYING
THE OHIO STATE UNIVERSITY
COLUMBUS, OHIO 43210

June 1988

SCIENTIFIC REPORT NO. 4

AIR FORCE GEOPHYSICS LABORATORY
AIR FORCE SYSTEMS COMMAND
UNITED STATES AIR FORCE
HANSCOM AIR FORCE BASE, MASSACHUSETTS 01731-5000

This technical report has been reviewed and is approved for publication.

CHRISTOPHER JEKELI
Contract Manager

THOMAS P. ROONEY, Chief
Geodesy & Gravity Branch

FOR THE COMMANDER

DONALD H. ECKHARDT, Director
Earth Sciences Division

This report has been reviewed by the ESD Public Affairs Office (PA) and is releasable to the National Technical Information Service (NTIS).

Qualified requestors may obtain additional copies from the Defense Technical Information Center. All others should apply to the National Technical Information Service.

If your address has changed, or if you wish to be removed from the mailing list, or if the addressee is no longer employed by your organization, please notify AFGL/DAA, Hanscom AFB, MA 01731-5000. This will assist us in maintaining a current mailing list.

Do not return copies of this report unless contractual obligations or notices on a specific document requires that it be returned.

Unclassified

SECURITY CLASSIFICATION OF THIS PAGE

REPORT DOCUMENTATION PAGE

Form Approved OMB No. 0704-0188

1a. REPORT SECURITY CLASSIFICATION Unclassified	1b. RESTRICTIVE MARKINGS
2a. SECURITY CLASSIFICATION AUTHORITY	3 DISTRIBUTION / AVAILABILITY OF REPORT Approved for public release; distribution Unlimited
2b. DECLASSIFICATION / DOWNGRADING SCHEDULE	
4. PERFORMING ORGANIZATION REPORT NUMBER(S) OSU/DGSS Report No. 393	5. MONITORING ORGANIZATION REPORT NUMBER(S) AFGL-TR-88-0199
6a. NAME OF PERFORMING ORGANIZATION Department of Geodetic Science and Surveying 6b. OFFICE SYMBOL (If applicable)	7a. NAME OF MONITORING ORGANIZATION Air Force Geophysics Laboratory
6c. ADDRESS (City, State, and ZIP Code) The Ohio State University Columbus, Ohio 43210	7b. ADDRESS (City, State, and ZIP Code) Hanscom AFB Massachusetts 01731-5000
8a. NAME OF FUNDING / SPONSORING ORGANIZATION 8b. OFFICE SYMBOL (If applicable)	9. PROCUREMENT INSTRUMENT IDENTIFICATION NUMBER F 19628-86-K-0016
8c. ADDRESS (City, State, and ZIP Code)	10. SOURCE OF FUNDING NUMBERS PROGRAM ELEMENT NO. 62101F; PROJECT NO. 7600; TASK NO. 03; WORK UNIT ACCESSION NO AQ

11. TITLE (Include Security Classification)
Downward Continuation of the Free-Air Gravity Anomalies to the Ellipsoid Using the Gradient Solution, Poisson's Integral and Terrain Correction-Numerical Comparison and Computations

12. PERSONAL AUTHOR(S)
Yan Ming Wang

13a. TYPE OF REPORT	13b. TIME COVERED	14. DATE OF REPORT (Year, Month, Day)	15. PAGE COUNT
Scientific No. 4	FROM _____ TO _____	1988 June	42

16. SUPPLEMENTARY NOTATION

17. COSATI CODES			18. SUBJECT TERMS (Continue on reverse if necessary and identify by block number)
FIELD	GROUP	SUB-GROUP	Geodesy; Gravity; Downward Continuation

19. ABSTRACT (Continue on reverse if necessary and identify by block number)

The formulas for the determination of the coefficients of the spherical harmonic expansion of the disturbing potential of the earth are defined for data given on a sphere. In order to determine the spherical harmonic coefficients, the gravity anomalies have to be analytically downward continued from the earth's surface to a sphere - at least to the ellipsoid. The goal of this work is to continue the gravity anomalies from the earth's surface downward to the ellipsoid using recent elevation models. The basic method for the downward continuation is the gradient solution (the g1 term). The terrain correction has also been computed because of the role it can play as a correction term when calculating harmonic coefficients from surface gravity data.

Because there is no global, dense gravity anomaly data, 5' x 5' mean elevation data has been used for the computations of the g1 term and the terrain correction on a global basis. The fast Fourier transformation has been applied to the computations.

The maximum g_1 term for the 5' x 5' mean blocks is located in the Himalaya Mountains

20 DISTRIBUTION / AVAILABILITY OF ABSTRACT	21 ABSTRACT SECURITY CLASSIFICATION
☐ UNCLASSIFIED/UNLIMITED ☐ SAME AS RPT ☐ DTIC USERS	Unclassified
22a. NAME OF RESPONSIBLE INDIVIDUAL Christopher Jekeli	22b TELEPHONE (Include Area Code) / 22c. OFFICE SYMBOL AFGL/LWG

DD Form 1473, JUN 86 *Previous editions are obsolete.* SECURITY CLASSIFICATION OF THIS PAGE

and has the magnitude of 442 mgals. The standard deviation is ± 2.56 mgals for the 5' x 5' mean block values. The terrain correction has the maximum value of 183 mgals, and standard deviation ± 1.01 mgals for 5' x 5' the mean block values.

The root mean square value of the degree variances of the correction terms, the g_1 term and the terrain correction, are about 2% of the degree variance of the disturbing potential. The root mean square effect of the geoid undulation due to the correction terms is about 0.7 meter for terms taken to degree 180. For the deflections of the vertical the correction terms contribute 0.1".

FOREWORD

This report was prepared by Dr. Wang Yan Ming, Research Assistant, Department of Geodetic Science and Surveying, The Ohio State University, under Air Force contract No. F19628-86-K-0016, OSU project No. 718188, Richard H. Rapp, Project Supervisor. The contract covering this research is administered by the Air Force Geophysics Laboratory, Hanscom Air Force Base, Massachusetts, with Dr. Christopher Jekeli, Scientific Program Officer.

Computer resources were provided by contract funds and by the Instruction and Research Computer Center.

ACKNOWLEDGMENT

I am very grateful to Dr. Richard H. Rapp, who supervised and reviewed the work and gave me various advice. I also thank Ms. Lisa Schneck for the typing of this report.

1. Introduction

The formulas for the determination of the coefficients of the spherical harmonics of the earth's gravitational potential require the free-air gravity anomalies to be given on a sphere, at least at a simple surface, e.g., the ellipsoid. Thus we have to continue the free-air gravity anomalies downward to a sphere or an ellipsoid.

The validity of the analytically downward continuation of the free-air gravity anomalies inside the earth is guaranteed by Runge's theorem (Moritz, 1980, p. 67). Of course these gravity anomalies are not the original gravity anomalies inside the earth. The downward continuation gives a fictitious gravity anomaly on the ellipsoid that generates a disturbing potential on and outside the earth that coincides with the original disturbing potential T on and outside the earth.

Moritz (1980) suggested that the free-air anomalies be continued to the point level. We can analytically take also the ellipsoid as the reference surface and use this method to continue the gravity anomalies down to the ellipsoid.

Bjerhammar (1964) suggested using the Poisson's integral to continue the free-air anomalies downward to a sphere embedded inside the earth. This problem was solved by using the discrete technique and matrix formulas.

Pellinen (1966) studied the methods for the determination of the coefficients of the spherical harmonics of the earth's gravitational potential and he added a term, which can be easily transformed into terrain correction, to the free-air gravity anomalies.

In this work we carry out some numerical investigation with the above mentioned methods. The terrain correction and the Molodensky's correction term g_1 are computed on a global basis.

2. Analytical Downward Continuation by Using Taylor Series

We continue the free-air gravity anomalies downward to a point level by using the Taylor series given by (Moritz, 1980, p. 378):

$$\Delta g = \Delta g' + z \frac{\partial \Delta g'}{\partial z} + \frac{1}{2!} z^2 \frac{\partial^2 \Delta g'}{\partial z^2} + \dots \qquad (1)$$

where $z = h - h_p$ is the elevation difference with respect to the computation point P, $\Delta g'$ is the gravity anomaly on the point level and Δg is the gravity anomaly on the earth's surface.

By using the up and downward continuation operators the correction terms of the gravity anomalies at the point level can be expressed as follows

$$\begin{aligned} g_1 &= -zL(\Delta g) \\ g_2 &= -zL(g_1) - \tfrac{1}{2}z^2 LL(\Delta g) \\ &\vdots \end{aligned} \qquad (2)$$

with

$$L(f) = \frac{R^2}{2\pi} \iint_{\sigma} \frac{f-f_p}{\ell_0^3} \, d\sigma \ , \tag{3}$$

where $\ell_0 = 2R\sin\psi/2$, ψ is the distance between the current point and the computation point P, σ is the unit sphere, and R is the mean radius of the earth.

If the ellipsoid is chosen as the reference surface, in other words, we want to have the reduced gravity anomalies not on the point level but on the ellipsoid, we have:

$$\begin{aligned} g_1 &= -hL(\Delta g) \\ g_2 &= -hL(g_1) - \tfrac{1}{2}h^2LL(\Delta g) \ , \\ &\vdots \end{aligned} \tag{4}$$

where h is the height of the topography above the ellipsoid.

Based on Runge's theorem the reference surface can be chosen arbitrarily for the downward continuation. One can show that the downward continuation of the gravity anomalies to the point level or to the ellipsoid is equivalent since they generate the same disturbing potential T on and outside the earth (cf. Sideris, 1987).

As a first approximation we have the gravity anomalies on the ellipsoid:

$$\Delta g^* = \Delta g + g_1 = \Delta g - hL(\Delta g) \tag{5}$$

This is called "gradient solution" (Moritz, 1966).

The relationship between the first correction term of the Molodensky's solution G_1 and g_1 is:

$$g_1 = G_1 - \frac{R^2}{2\pi} \iint_{\sigma} \frac{h\Delta g - h_p\Delta g_p}{\ell_0^3} \, d\sigma \ . \tag{6}$$

The first correction term of the Molodensky's solution is given by

$$G_1 = \frac{R^2}{2\pi} \iint_{\sigma} \frac{h-h_p}{\ell_0^3} \, \Delta g d\sigma \ . \tag{7}$$

After some reordering, equation (6) can be changed into

$$g_1 = G' - \frac{R^2}{4\pi} \iint_{\sigma} \frac{(\Delta g-\Delta g_p)(h-h_p)}{\ell_0^3} \, d\sigma \ , \tag{8}$$

where G' is the term which was suggested by Pellinen (1966, p. 70):

$$G' = \frac{R^2}{4\pi} \iint_{\sigma} \frac{(\Delta g-\Delta g_p)(h-h_p)}{\ell_0^3} \, d\sigma \ . \tag{9}$$

If we assume there is a linear relationship between the gravity anomaly and the elevation:

$$\Delta g = a + bh, \quad b = 2\pi k\rho \ , \tag{10}$$

where a is a constant, k the gravitational constant and ρ the density of the crust, then eqn. (9) becomes

$$G' = C = \frac{1}{2} k\rho R^2 \iint_\sigma \frac{(h-h_p)^2}{\ell_0^3} \, d\sigma \ , \tag{11}$$

where C denotes the terrain correction.

Equation (8) can be written in the form

$$g_1 = C - \frac{1}{2} k\rho R^2 \iint_\sigma \frac{h^2-h_p^2}{\ell_0^3} \, d\sigma \ . \tag{12}$$

Equation (12) gives the relationship between the first correction term of Moritz's solution with the terrain correction. Moritz (1966, p. 106) shows that the terrain correction plays a role in the estimation of the low degrees of the spherical harmonics of the earth's gravitational potential, using surface gravity data. But the last integral in (12) cannot be neglected if the high degrees of the spherical harmonics are determined.

From the equations (11) and (12) we get

$$g_1 = -k\rho R^2 h_p \iint_\sigma \frac{h-h_p}{\ell_0^3} \, d\sigma \ . \tag{13}$$

We can get equation (13) directly from:

$$g_1 = -h_p L(\Delta g) = -h_p \frac{R^2}{2\pi} \iint_\sigma \frac{\Delta g - \Delta g_p}{\ell_0^3} \, d\sigma \tag{14}$$

under the assumption (10).

The formulas (11) and (13) have the advantage that they can be evaluated from topograghy only, no gravity anomalies being needed. The weakness is that one has to make the assumption (10).

In a plane approximation, eqns. (11) and (13) become

$$g_1 = -h_p \, k\rho \iint_\tau \frac{h-h_p}{\ell_0^3} \, dxdy \ , \tag{15}$$

$$C = \tfrac{1}{2} k\rho \iint_\tau \frac{(h-h_p)^2}{\ell_0^3} \, dxdy \tag{16}$$

with $\ell_0 = [(x-x_p)^2 + (y-y_p)^2]^{\frac{1}{2}}$, where τ is the two-dimensional plane.

3. Downward Continuation of the Free-Air Gravity Anomalies Using the Poisson's Integral

Another method for the downward continuation of the gravity anomalies to the ellipsoid is using the Poisson's Integral (Moritz, 1966, sec. 7). In the plane approximations we have:

$$\Delta g^*_p = \Delta g_p - \frac{h_p}{2\pi} \iint_\tau \frac{\Delta g^* - \Delta g^*_p}{\ell^3} \, dxdy \ , \tag{17}$$

where Δg^*, Δg are the gravity anomalies on the ellipsoid and on the earth's surface respectively. The distance between the computation point P on the earth's surface and the current point on the ellipsoid is

$$\ell = [(x-x_p)^2 + (y-y_p)^2 + h_p^2]^{1/2} \ . \tag{18}$$

If we introduce the identical operator I and the operator L_p

$$If = f \tag{19}$$

$$L_p f = \frac{h_p}{2\pi} \iint_\tau \frac{f - f_p}{\ell^3} \, dxdy \ . \tag{20}$$

Then eqn. (17) can be written in the form

$$(I + L_p)\Delta g^* = \Delta g \ . \tag{21}$$

Its solution is given by

$$\begin{aligned} \Delta g^* &= (I + L_p)^{-1} \Delta g \\ &= \sum_{n=0}^{\infty} (-1)^n L_p^n \, \Delta g \\ &= \sum_{n=0}^{\infty} g^*_n \end{aligned} \tag{22}$$

with

$$g^*_n = (-1)^n L_p^n \Delta g \ . \tag{23}$$

More explicitly we write

$$\begin{aligned} g^*_0 &= \Delta g \\ g^*_1 &= -L_p \Delta g = -\frac{h_p}{2\pi} \iint_\tau \frac{\Delta g - \Delta g_p}{\ell^3} \, dxdy \\ g^*_2 &= L_p^2 \Delta g = -L_p g^*_1 = -\frac{h_p}{2\pi} \iint_\tau \frac{g^*_1 - g^*_{1p}}{\ell^3} \, dxdy \\ &\vdots \end{aligned} \tag{24}$$

Comparing g^*_2 in (24) with (14), we find that both formulas are similar. The difference is that the integral kernel for g^*_2 is ℓ^{-3} and for g_1 is ℓ_0^{-3}. It was shown (Moritz, 1966, p. 60) that the formulas for g^*_2 and g_1 are approximately equivalent. g^*_2 will give more accurate results.

4. Some Considerations About Applying the FFT Technique to the Poisson's Integral

The FFT (Fast Fourier Transformation) is widely used for numerical computations. We consider here how the FFT technique can be used for P-integral (Poisson's integral). This work has been described by Euler et al. (1980), but we have to recognize that the Fourier transformation can not be directly used for the P-integral in plane approximation due to the elevation variable which is included in the kernel of the P-integral. We have to do some things before we apply the FFT to the P-integral.

In plane approximation the P-integral becomes

$$\Delta g_p = \frac{h_p}{2\pi} \iint_\tau \frac{\Delta g^*}{\ell^3}\, dxdy \tag{25}$$

where Δg_p is the gravity anomaly at point P which is located on the earth's surface, Δg^* is the gravity anomaly on the ellipsoid, h_p is the elevation of the point P. The distance between point P and the current point on the ellipsoid is

$$\ell = \sqrt{(x-x_p)^2+(y-y_p)^2+h_p^2} \tag{26}$$

Because the elevation variable, h_p, is included in the kernel ℓ^{-3}, the kernel can not be written in the form

$$\ell = \ell(x_p,y_p,x,y,h(x_p,y_p)) = \ell(x-x_p,y-y_p)$$

and the P-integral is not a convolution. The definition of the two dimensional convolution is given in Bracewell (1965, p. 243).

The two dimensional Fourier transformation and its inverse are defined as:

$$F(u,v) = \mathcal{F}\{f(x,y)\} = \iint_{-\infty}^{\infty} f(x,y)e^{-2\pi i(xu+yv)}dxdy \tag{27}$$

$$f(x,y) = \mathcal{F}^{-1}\{F(u,v)\} = \iint_{-\infty}^{\infty} F(u,v)e^{2\pi i(xu+yv)}dudv \tag{28}$$

where the symbols $\mathcal{F}$, $\mathcal{F}^{-1}$ denote the Fourier transformation and its inverse.

If the elevation h_p is constant in the integration region, the integral (25) can be considered as a convolution. Apply the Fourier transformation to (25) and we get immediately (Euler, et. al., 1986)

$$G(u,v) = e^{-2\pi h_p w}G^*(u,v) \tag{29}$$

with $w = \sqrt{u^2+v^2}$, u,v are the frequency variables, G and G* are the Fourier transformations of the gravity anomalies Δg, Δg^* respectively.

From (29) we have

$$G^*(u,v) = e^{2\pi h_p w}G(u,v) \tag{30}$$

(30) shows that the gravity anomaly on the ellipsoid is rougher than the gravity anomaly on the earth's surface. Although the relationship of the spectra of the gravity anomalies Δg and Δg^* is really not so simple as (30) shows, the relationship of the spectra of the gravity anomalies should have similar properties: the upward continuation makes the gravity anomalies smoother and the downward continuation makes the gravity anomalies rougher. We have to see that if we have some observation errors in the gravity anomalies, and normally the errors are assumed to be composed of high frequencies, e.g., the white noise, then the downward continuation enlarges the spectra of the errors by the factor $\exp(2\pi h_p \omega)$. This means, a small error in Δg can cause a big error in Δg^*, if the errors in Δg are composed of high frequencies. Therefore the downward continuation may not be stable. The situation is not so serious in practice if we use the mean block values which may decrease the effect of the high frequencies in the errors.

Now we go back to see how we can apply the Fourier transformation to the P-integral.

For the Kernel function ℓ^{-3}, we have

$$\begin{aligned} \ell^2 &= (x-x_p)^2 + (y-y_p)^2 + h_p^2 \\ &= (x-x_p)^2 + (y-y_p)^2 + C + (h_p^2 - C^2) \\ &= S^2 + (h_p^2 - C^2) , \end{aligned} \tag{31}$$

with

$$S^2 = (x-x_p)^2 + (y-y_p)^2 + C^2 ,$$

C is a constant. If we take $C = h_{max}$, the maximum of the elevation in the integration region, we have

$$\ell^2 = S^2\left(1 + \frac{h_p^2 - h_{max}^2}{S^2}\right) = S^2\left(1 + \frac{H}{S^2}\right) , \tag{32}$$

with

$$H = h_p^2 - h_{max}^2$$

The P-integral is expanded into the series

$$\Delta g_p = \frac{h_p}{2\pi} \iint_\tau \frac{\Delta g^*}{S^3}\left(1 - \frac{3}{2}\frac{H}{S^2} + \frac{15}{8}\frac{H^2}{S^4} - \frac{105}{48}\frac{H^3}{S^6} + \ldots\right) dxdy . \tag{33}$$

Because we have always

$$\left|\frac{H}{S^2}\right| < 1$$

the series in the integral (33) converges absolutely.

Now we apply the Fourier transformation to (33)

$$\Delta g_p = \frac{h_p}{2\pi}\left[\mathcal{F}^{-1}\{G^*\mathcal{F}\{\frac{1}{S^3}\}\} - \frac{3}{2} H\mathcal{F}^{-1}\{G^*\mathcal{F}\{\frac{1}{S^5}\}\} + \frac{15}{8} H^2\mathcal{F}^{-1}\{G^*\mathcal{F}\{\frac{1}{S^7}\}\}\ldots\right] \tag{34}$$

For the kernel $S^{-(2n+1)}$ we have

$$S^{-(2n+1)} = (-\frac{2}{1})(-\frac{2}{3})\ldots(-\frac{2}{2n-1})\frac{\partial^n}{\partial(h_{max}^2)^n}(\frac{1}{S})$$

$$n=1,2,\ldots \tag{35}$$

The Fourier transform of the kernel S^{-1} is (Bracewell, 1965, p.249):

$$\mathcal{F}\{\frac{1}{S}\} = \frac{1}{\omega} e^{-2\pi h_{max}\omega} . \tag{36}$$

By using eqns. (35) and (36) we have

$$\mathcal{F}\{\frac{1}{S^3}\} = -2\frac{\partial}{\partial(h_{max}^2)}\mathcal{F}\{\frac{1}{S}\} = \frac{2\pi}{h_{max}} e^{-2\pi h_{max}\omega} \tag{37}$$

$$\mathcal{F}\{\frac{1}{S^5}\} = \frac{4}{3}\frac{\partial^2}{\partial(h^2_{max})^2}\mathcal{F}\{\frac{1}{S}\} = \frac{2\pi}{3h^2_{max}}(\frac{1}{h_{max}} + 2\pi\omega) e^{-2\pi h_{max}\omega}, \tag{38}$$

then (34) becomes

$$\Delta g_p = h_p[\mathcal{F}^{-1}\{G^* \frac{1}{h_{max}} e^{-2\pi h_{max}\omega}\} - \frac{H}{2h^2_{max}} \mathcal{F}^{-1}\{G^*(\frac{1}{h_{max}} + 2\pi\omega) e^{-2\pi h_{max}\omega} + \ldots] \tag{39}$$

Equations (34) and (39) have more theoretical meaning because the series converges slowly. Numerical tests show that if a 1 mgal accuracy of the P-integral is needed, the computation should include up to the fifth term in the series (34).

In order to increasse the convergence of the series we modify this method. We decompose the integral kernel ℓ^{-3} into two parts:

$$\ell^{-3} = \ell_I^{-3} + \ell_{II}^{-3} \tag{40}$$

with

$$\ell_I^{-3} = \begin{cases} \ell^{-3} & x,y \in D \\ 0 & x,y \notin D \end{cases} \tag{41}$$

$$\ell_{II}^{-3} = \begin{cases} 0 & x,y \in D \\ \ell^{-3} & x,y \notin D \end{cases} \tag{42}$$

where D is the innermost zone surrounding the point P.

Now the P-integral is decomposed into two integrals:

$$\Delta g_p = \frac{h_p}{2\pi}\iint_\tau \frac{\Delta g^*}{\ell_I^3} dxdy + \frac{h_p}{2\pi}\iint_\tau \frac{\Delta g^*}{\ell_{II}^3} dxdy \tag{43}$$

We expand the second integral in the series as

$$\frac{h_p}{2\pi}\iint_\tau \frac{\Delta g^*}{\ell_{II}^3} dxdy = \frac{h_p}{2\pi}\iint_\tau \frac{\Delta g^*}{S_{II}^3}(1 - \frac{3}{2}\frac{H}{S_{II}^3} + \frac{15}{8}\frac{H^2}{S_{II}^4} - \ldots) dxdy \tag{44}$$

with

$$S_{II} = \begin{cases} S & x,y \in D \\ 0 & x,y \notin D \end{cases} \tag{45}$$

The integrals in (44) are not difficult to compute by the use of the Fourier transformation or FFT technique. If the innermost zone D is properly chosen, the series (44) converges very fast. We give a numerical test hereafter.

For the first integral in (43) the numerical integration is used. Because the integral is only evaluated in the innermost zone, the computation can be completed fast.

Now we give a numerical test for the above mentioned methods.

We simulate the gravity anomalies data on the ellipsoid by using the formula

$$\Delta g^* = 0.11h - 200. \tag{46}$$

where h is in meter; Δg^* in mgals.

The digital elevation at 30" grid interval for the USA is used. The extent of the test region is 50 x 50 km. In this region the maximum elevation is 3260 meters; the lowest elevation is 1830 meters and the mean elevation is 2374 meters. Values have been computed for points located in a rectangle in the center of the area where the points are approximately 1 km apart.

Results for Δg_p from (34) up to the fourth term are given in Table 1. The numerical integration values of the P-integral are also given as the check values.

Table 1. Results for Δg_p from (34) (Unit: mgal)

Point number	1	2	3	4
1st term	41.11	41.64	38.71	37.89
2nd term	10.48	10.43	11.01	11.20
3rd term	3.53	3.44	4.16	4.39
4th term	1.32	1.28	1.74	1.90
Sum (Δg_p)	56.44	56.77	55.62	55.38
Check Values	57.25	57.53	56.68	56.78
Sum-Check Val.	-0.81	-0.76	-1.06	-1.40
Δg^*	66.20	68.40	53.00	47.50

Table 1 shows the series (34) numerically converges with factor 1/3 approximately in the test region. If we want to have the computing accuracy at 1 mgal, we have to complete the computations up to the 5th term of the series.

We now give the results for Δg_p from (43) and (44) in Table 2. The innermost zone is chosen as a 5'x5' square and the P-integral is completed in this square with numerical integration. The FFT technique is applied to (44).

Table 2. Results for Δg_p from (43) and (44). (Unit:mgal)

Point number	1	2	3	4
Innermost Zone	39.91	40.05	40.02	40.40
1st term (eq.(44))	16.25	16.38	15.71	15.32
2nd term	1.07	1.06	1.17	1.19
3rd term	0.08	0.08	0.10	0.11
4th term	0.01	0.01	0.01	0.01
Sum	57.32	57.58	57.01	57.03
Check Values	57.25	57.53	56.68	56.68
Sum-check Values	0.07	0.05	0.33	0.25
Δg^*	66.20	68.40	53.00	47.50

Table 2 shows the series (44) converges very fast. Even when we choose a small innermost zone (5'x5' square), the computations for the series (44) need only the first and second term.

We give a short summary about the use of FFT for the P-integral. We can use FFT through the computation of (34). The disadvantage is that the series converges slowly. The numerical test shows if we want to have computing accuracy at 1 mgal, we have to compute the series (34) up to the 5th term. In the modified method we separate the integration region into two parts: innermost zone and outer zone. We evaluate the P-integral in the innermost zone with numerical integration. The innermost zone is chosen small and this computation is not time consuming. Equation (44) is used for computing the P-integral in the outer zone. For the numerical computation, eqns. (43) and (44) are more beneficial than (34).

In these procedures there are several concerns. First, we must understand why FFT calculations near the boundaries of the data area give incorrect results as has been demonstrated by Sideris (1985, p. 70, Figure 1). In addition we must consider how mean block values can be used in the FFT computations.

The integrals in physical geodesy are defined on a sphere or approximated in a plane. In practice the integrals are evaluated in a limited region. Generally we write

$$g(x_p,y_p) = \int_0^a \int_0^b f(x,y)\ k(x,y,x_p,y_p)\ dxdy \qquad (47)$$

where $k(x,y,x_p,y_p)$ is the integral kernel. If the kernel satisfies the condition

$$k(x,y,x_p,y_p) = k(x-x_p,y-y_p) \qquad (48)$$

then the discrete Fourier transformation can be used for (47). Here we consider only this case.

In order to use the FFT technique, we first have to discretize the integral in (47) in the form:

$$g_p = \sum_{m=o}^{N1-1} \sum_{n=o}^{N2-2} f(m\Delta x, n\Delta y)\, k(m\Delta x - x_p, n\Delta y - y_p)\, \Delta x \Delta y \qquad (49)$$

where $\Delta x, \Delta y$ are the variable increments, N1, N2 are the grid point numbers in the integration region along x,y directions.

Setting

$$\begin{cases} x_p = r\Delta x & r = 0,1,\ldots N1-1 \\ y_p = s\Delta y & s = 0,1,\ldots N2-1 \end{cases} \qquad (50)$$

(49) becomes

$$g_p = \sum_{m=o}^{N1-1} \sum_{n=o}^{N2-1} f(m\Delta x, n\Delta y)\, k[(m-r)\Delta x, (n-s)\Delta y]\, \Delta x \Delta y \qquad (51)$$

If we want to apply FFT to (51), we have to extend the function f and the kernel k into the whole plane as follows:

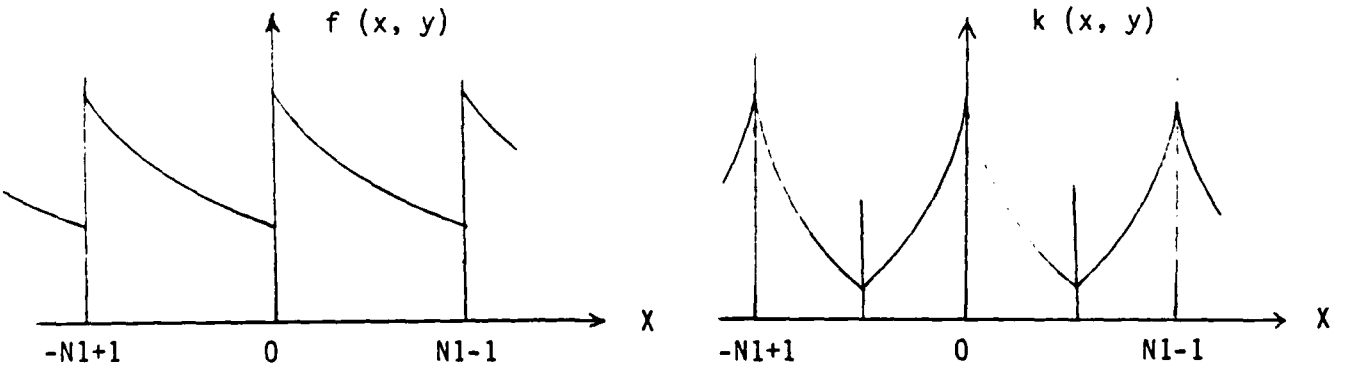

Figure 1. Periodic extension of the function f and kernel k, (y = 0)

This periodic extension means we now have

$$\begin{aligned} f[(m+N1)\Delta x, (n+N2)\Delta y] &= f(m\Delta x, n\Delta y) \\ k[(m+N1)\Delta x, (n+N2)\Delta y] &= k(m\Delta x, n\Delta y) \end{aligned} \qquad (52)$$

Here we must recognize that this extension causes errors in the computations because the function f and the kernel k are not periodic.

The discrete Fourier transformation and its inverse are defined as

$$F(m\Delta u, n\Delta v) = \sum_{k=0}^{N1-1} \sum_{\ell=0}^{N2-1} f(m\Delta x, n\Delta y) e^{2\pi i (\frac{km}{N1} + \frac{\ell n}{N2})} \tag{53}$$

$$f(k\Delta x, \ell\Delta y) = \frac{1}{N1N2} \sum_{m=0}^{N1-1} \sum_{n=0}^{N2-1} F(m\Delta u, n\Delta v) e^{-2\pi i (\frac{km}{N1} + \frac{\ell n}{N2})} \ . \tag{54}$$

The discrete Fourier transformation of (51) is

$$G(m\Delta u, n\Delta v) = \sum_{k,\ell} g_p(k\Delta x, \ell\Delta y) e^{2\pi i (\frac{km}{N1} + \frac{\ell n}{N2})}$$

$$= \sum_{k,\ell} \sum_{r,s} f(r\Delta x, s\Delta y) k[(r-k)\Delta x, (s-\ell)\Delta y] e^{2\pi i (\frac{km}{N1} + \frac{\ell n}{N2})\Delta x\Delta y} \tag{55}$$

Setting

$$\begin{cases} r - k = g & g = -N1+\ell+r, \ldots, r \\ s - \ell = h & h = -N2+\ell+s, \ldots, s \end{cases} , \tag{56}$$

(55) becomes

$$G(m\Delta u, n\Delta v) = \sum_{r,s} f(r\Delta x, s\Delta y) e^{2\pi i (\frac{rm}{N1} + \frac{sn}{N2})}$$

$$\cdot \sum_{k,\ell} k(g\Delta x, h\Delta y) e^{-2\pi i (\frac{gm}{N1} + \frac{hn}{N2})\Delta x\Delta y} \tag{57}$$

$$= F(m\Delta u, n\Delta v) K(m\Delta u, n\Delta v) \Delta x\Delta y \ ,$$

where

$$F(m\Delta u, n\Delta v) = \sum_{r=0} \sum_{s=0} f(r\Delta x, s\Delta y) e^{2\pi i (\frac{rm}{N1} + \frac{sn}{N2})} \ , \tag{58}$$

$$K(m\Delta u, n\Delta v) = \sum_{k,\ell} k(g\Delta x, h\Delta y) e^{-2\pi i (\frac{gm}{N1} + \frac{hn}{N2})}$$

$$= \sum_{g=r}^{r-N1+1} \sum_{h=s}^{s-N2+1} k(g\Delta x, h\Delta y) e^{-2\pi i \left(\frac{gm}{N1} + \frac{hn}{N2}\right)} \quad . \tag{59}$$

If the kernel is periodic as (52) shows, we have immediately

$$K(m\Delta u, n\Delta v) = \sum_{g=0}^{N1-1} \sum_{h=0}^{N2-1} k(g\Delta x, h\Delta y) e^{2\pi i \left(\frac{gm}{N1} + \frac{hn}{N2}\right)} \quad . \tag{60}$$

It is not the case in the numerical integration because the kernel function is not periodic. In order to see this more specifically, we give an example. We take the kernel

$$k(x,y) = s^{-3}$$
$$= (x^2 + y^2 + h_{max}^2)^{3/2}$$

Figure 2 represents the kernel k and its periodic extension.

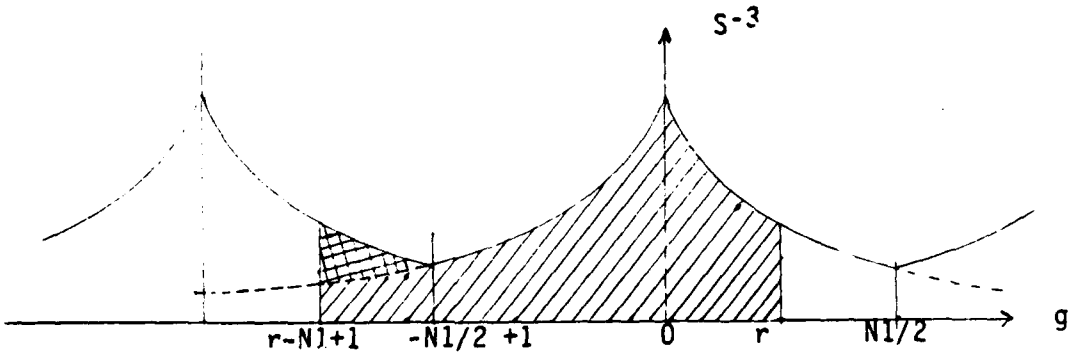

Figure 2. Kernel k and its periodic extension

The striped part is the range of the kernel s^{-3} in (59). If we use (60), then the range of the kernel s^{-3} is the striped part plus the shaded part. The shaded part is the error caused by making the kernel function periodic. At r=0, corresponding to the boundary point, the errors will go to the largest (see Figure 2). Therefore the boundary values of the FFT computations are wrong.

We can see that only at the center of the integration region, where

$$r = \frac{N1}{2} \quad \text{and} \quad s = \frac{N2}{2} \ ,$$

do we have equation (59) equal to (60). The closer the computation points are to the center, the smaller the shaded part in Figure 2, or, the smaller the error caused by extending the kernel function periodically.

In the FFT computations we use (60) instead of (59). Based on the above discussion we know only at the center point there are no errors caused by extending the kernel function periodic. The situation is not so serious if the kernel function decreases very fast, e.g., ℓ_0^{-3} or s^{-3}, as in this case, the errors are small if the computation points are not at the boundary region (cf. Sideris, 1985,p. 70, Fig. 1). What we have to remember is that we take a proper boundary for the computations in order to guarantee the computations are sufficiently accurate.

This problem seems more serious for applying FFT to the Stokes integral, because the kernel ℓ_0^{-1} decreases slowly. If the boundary is not correctly taken, the errors may be significant. In other words, the boundary has to be chosen large enough.

In order to decrease the errors caused by extending the kernel function periodic, we can enlarge the integration region by putting a zero boundary—some zero values are assigned to the function f in the added boundary. Now we consider how we can use the block mean values for the FFT computations.

If the function f is given in mean block values, then the integral (47) becomes

$$g(x_p,y_p) = \int_0^a \int_0^b f(x,y)k(x-x_p,y-y_p)dxdy$$

$$= \sum_{i,j} \bar{f}(i\Delta x, j\Delta y) \int\int_{\Delta ij} k(x-x_p,y-y_p)dxdy \qquad (61)$$

where $\bar{f}(i\Delta x,j\Delta y)$ is the mean block values of the function f in the block Δij.

We denote the integral in (61) by c and put (50) in this integral

$$c[(i-r)\Delta x,(j-s)\Delta y] = \int\int_{\Delta ij} k(x-x_p,y-y_p)dxdy$$

$$= \int_{(i-\frac{1}{2})\Delta x}^{(i+\frac{1}{2})\Delta x} \int_{(j-\frac{1}{2})\Delta y}^{(j+\frac{1}{2})\Delta y} k(x-r\Delta x,y-s\Delta y)\, dxdy \qquad (62)$$

then (61) becomes

$$g(r\Delta x,s\Delta y) = \sum_{i,j} \bar{f}(i\Delta x,j\Delta y)\ c[(i-r)\Delta x,(j-s)\Delta y] \qquad (63)$$

The discrete Fourier transformation of (63) is

$$G(k\Delta u,l\Delta v) = \bar{F}(k\Delta u,l\Delta v)\ C(k\Delta u,l\Delta v) \qquad (64)$$

where $\bar{F}$, C are the discrete Fourier transforms of the mean values $\bar{f}$ and the kernel function c, respectively.

Taking the inverse of the discrete Fourier transformation of eqn. (64), we get

$$g(r\Delta x, s\Delta y) = \sum_{k=0}^{N1-1} \sum_{l=0}^{N2-1} G(k\Delta u, l\Delta v) e^{-2\pi i \left(\frac{kr}{N1} + \frac{ls}{N2}\right)} \frac{1}{N1 \cdot N2}$$

$$= \frac{1}{N1N2} \sum_{k=0}^{N1-1} \sum_{l=0}^{N2-1} \overline{F}(k\Delta u, l\Delta v) C(k\Delta u, l\Delta v) e^{-2\pi i \left(\frac{kr}{N1} + \frac{ls}{N2}\right)} \quad (65)$$

We point out that we consider the FFT technique only as a computing tool. With its help we can evaluate (63) very fast. Equations (64) and (65) give the same results as (63), except for some errors caused by extending the kernel function periodically.

5. Numerical Investigation of the Downward Continuation - A Comparison of Downward Continuation by Using the Gradient Solution and Terrain Correction

The downward continuation of the gravity anomalies to the ellipsoid by using the gradient solution, Poisson's integral and the terrain correction require a dense distribution of gravity anomaly data and elevation data surrounding the computation point. If we use the mean block values in the integration, the small block size will be needed for a high computational accuracy. Up to date the mean free-air anomaly in 30' block and the mean elevation in 5' block are given in a global basis. The mean free-air anomaly in 30' block is not suitable for the above mentioned integrals.

The digital elevation at 30" grid interval for the U.S. is available. We will use this data for the computation of (15) and (16). From the results the mean block values of the gradient solution g_1 and the terrain correction (TC) in 5' and 30' block sizes will be formed. The 5'x5' mean elevation will be formed by averaging the 30" point elevation and are used for the computations of (15) and (16). We want to see what happens if the bigger mean block values are used.

The tests are taken in three different topographic regions. In the region $36^\circ \leq \phi \leq 37^\circ$, $241^\circ \leq \lambda \leq 242^\circ$ the topography varies from 200 meters to 3600 meters; in the region $39^\circ \leq \phi \leq 40^\circ$, $253^\circ \leq \lambda \leq 254^\circ$ the topography ranges from 2100 meters to 3100 meters; in the region $35^\circ \leq \phi \leq 36^\circ$, $277^\circ \leq \lambda \leq 278^\circ$ the topography varies from 250 meters to 1400 meters.

The g_1 term and the terrain correction are given in Table 3-8 for the test regions. The maximum of the g_1 term in a 5'x5' mean block is 70 mgals in the rough area ($36^\circ \leq \phi \leq 37^\circ$, $241^\circ \leq \lambda \leq 242^\circ$), and the minimum of the g_1 term is -28 mgals ($39^\circ \leq \phi \leq 40^\circ$, $253^\circ \leq \lambda \leq 254^\circ$). The maximum of the terrain correction in a 5'x5' mean block is 22 mgals ($36^\circ \leq \phi \leq 37^\circ$, $241^\circ \leq \lambda \leq 242^\circ$).

37°

17	25	- 6	9	-13	26	34	41	-15	-12	18	54
-5	10	16	39	40	13	11	55	- 9	-11	- 9	24
20	2	-10	-10	- 9	- 5	16	55	-16	-11	-10	27
12	18	22	16	- 1	17	40	62	8	-13	- 9	- 2
- 2	3	7	34	38	28	21	24	70	-19	- 7	-11
2	- 1	- 3	- 9	-15	40	50	- 2	58	57	- 9	- 9
1	- 2	2	5	13	38	1	12	15	34	37	11
0	- 1	5	18	34	21	25	- 5	4	3	40	- 2
- 1	9	9	20	34	- 8	32	4	29	9	43	-10
0	0	- 5	6	11	10	- 8	- 8	12	2	19	3
0	- 1	- 1	15	0	12	- 8	- 9	6	16	8	18
- 1	- 1	- 1	- 5	9	5	- 4	35	16	4	0	21

36° 241° 242°

a) 5'x5' Mean Values

10	15
7	10

b) 30'x30' Mean Values

10

c) 1°x1° Mean Value

Table 3. g_1 in 5', 30' and 1° Mean Block Values (30" Point Elevation Data)

37°

8	8	11	17	15	11	11	19	11	7	10	13
19	18	19	13	10	14	11	16	14	7	7	12
8	9	13	12	14	17	13	16	13	7	6	14
7	7	7	7	8	11	11	14	19	8	5	11
6	9	7	11	11	11	11	9	20	13	6	6
6	10	12	14	14	11	12	11	14	22	12	6
6	9	11	13	12	10	9	10	6	9	16	9
5	7	11	12	9	11	11	8	4	5	13	11
4	7	10	12	10	6	10	9	6	4	13	11
4	5	7	9	10	5	5	8	5	3	7	9
4	5	9	11	9	6	6	7	4	3	5	10
4	5	7	8	8	6	8	7	4	3	4	9

36° 241° 242°

a) 5'x5' Mean Values

11	12
8	8

b) 30'x30' Mean Values

10

c) 1°x1° Mean Value

Table 4. TC in 5', 30' and 1° Mean Block Values (30" Point Elevation Data)

40°

- 5	16	0	-9	7	-22	4	-12	14	-10	5	3
- 9	-17	-16	- 4	- 4	21	4	- 1	-19	20	- 1	- 3
- 9	29	23	1	- 5	- 9	7	40	21	-18	12	6
- 4	- 4	- 1	-10	3	23	2	9	36	19	-15	28
-17	-13	-17	2	-17	-18	-14	- 5	-12	29	6	-19
11	16	6	4	26	24	1	- 7	12	4	- 3	-13
27	27	21	11	18	15	36	-10	- 4	20	27	-15
- 9	- 3	-15	-17	- 5	15	1	11	15	- 1	38	20
-12	-13	20	24	-13	9	9	- 7	- 2	19	13	- 1
- 2	-18	- 5	- 1	15	22	30	-20	-11	30	18	- 6
29	2	0	12	11	29	36	-13	-14	30	2	- 2
15	36	- 2	-13	36	6	20	4	-28	12	11	1

39° 253° 254° 106°

a) 5'x5' Mean Values

0	4
8	7

b) 30'x30' Mean Values

5

c) 1°x1° Mean Value

Table 5. g_1 in 5', 30' and 1° Mean Block Values (30" Point Elevation Data)

40°

2	3	3	3	3	3	3	2	3	2	1	2
3	4	3	4	4	5	4	3	3	5	2	3
4	4	4	2	3	4	4	6	7	4	3	5
2	3	4	3	4	4	3	4	7	6	3	6
4	4	3	3	4	5	5	5	6	5	4	3
9	5	5	4	5	7	5	5	3	3	6	2
6	6	5	4	5	7	7	4	4	3	5	3
6	7	7	5	3	5	5	3	3	3	4	5
4	4	5	4	5	4	4	2	3	5	5	2
6	5	6	4	5	6	5	2	2	5	4	7
9	10	7	7	5	5	8	3	2	4	3	1
10	13	7	4	6	6	9	9	4	4	3	1

39° 253° 254° 106°

a) 5'x5' Mean Values

4	4
6	4

b) 30′ x 30′ Mean Values

5

c) 1° x 1° Mean Value

Table 6. TC in 5', 30' and 1° Mean Block Values (30" Point Elevation Data)

40°

1	1	3	-1	6	7	6	0	0	1	1	4
3	1	0	3	2	2	0	3	6	-1	5	0
8	2	4	-1	-1	-2	-1	10	16	1	3	-2
1	7	2	-1	-1	0	8	10	15	5	1	1
1	5	5	1	0	1	-1	-1	6	-2	-1	0
-1	0	1	-2	-1	-1	2	6	2	2	2	1
5	1	4	2	1	-1	-1	4	2	1	-1	0
10	14	5	4	-1	-1	1	-1	4	-1	0	0
10	8	0	0	0	1	0	0	2	2	0	0
3	0	-1	1	0	4	3	1	3	-1	0	0
4	1	2	5	4	1	-1	1	-1	0	0	0
0	2	2	1	-1	0	0	0	0	0	0	0

39° 253° 254° 106°

a) 5'x 5' Mean Values

2	3
3	1

b) 30′ x 30′ Mean Values

2

c) 1° x 1° Mean Value

Table 7. g_1 in 5, 30' and 1° Mean Block Values (30" Point Elevation Data)

36°

2	2	2	2	3	2	3	2	2	1	1	2
3	3	2	1	1	1	1	2	4	2	2	2
3	2	2	1	1	1	2	4	7	3	3	2
2	3	2	1	0	1	3	6	6	4	3	1
2	3	3	1	1	1	2	3	2	2	1	1
1	1	2	1	1	0	1	2	1	2	2	1
3	2	3	2	1	0	1	2	3	2	1	1
5	5	3	2	1	0	1	0	0	1	0	0
3	4	2	1	1	1	0	1	2	1	0	0
2	1	1	1	1	2	1	1	2	1	0	0
2	1	1	1	2	2	1	1	1	0	0	0
2	2	2	2	1	1	0	0	0	0	0	0

35° 277° 278°

a) 5'× 5' Mean Values

2	3
2	1

b) 30′× 30′ Mean Values

2

c) 1°× 1° Mean Value

Table 8. TC in 5' , 30' and 1° Mean Block Values
(30" Point Elevation Data)

From the above Tables, we see that the correction term g_1 has large differences with the terrain corrections in the 5'× 5' mean block values. The results in bigger mean block values agree better. The mean block values of g_1 agree very well with the mean terrain correction in 1°x1° block.

We also use the mean elevation in 5'x5' block formed by averaging the 30" point elevation data for the computations of (15) and (16). The results are given in Tables 9 and 10.

40°

- 3	10	- 3	- 9	1	-18	1	-10	5	- 7	- 6	2
-11	-16	-12	- 7	- 9	10	4	0	-14	9	3	0
- 9	23	18	- 1	- 6	- 5	6	29	12	-14	- 8	2
- 5	- 5	- 4	-11	- 4	13	0	6	29	14	-14	15
-15	-13	-16	- 2	-15	-16	-13	- 6	- 8	21	- 1	-16
3	9	0	- 2	17	19	- 1	- 8	9	5	- 2	-13
21	17	14	7	15	20	20	-11	- 2	12	16	- 7
- 9	- 4	- 8	-13	- 7	12	4	7	6	5	30	16
-14	12	11	11	-12	4	9	- 7	- 3	17	14	1
3	-17	- 9	4	16	15	17	-16	-10	24	16	- 4
22	- 3	- 5	6	8	20	21	-13	-13	23	5	- 4
16	25	- 3	13	23	7	12	1	-20	6	12	0

39° 253° 254° 106°

a) 5'× 5' Mean Values

-3	1
5	5

b) 30′× 30′ Mean Values

2

c) 1°× 1° Mean Value

Table 9. g_1 in 5', 30' and 1° Mean Block Values
(5' Mean Elevation Data)

40'

1	1	1	1	1	2	1	1	1	1	1	1
2	2	1	1	1	1	1	1	2	1	1	1
1	2	2	1	1	1	1	3	2	2	1	1
1	1	1	1	1	1	1	1	2	2	1	1
2	2	2	1	2	2	1	1	1	2	1	1
1	2	1	1	2	2	1	1	1	1	1	1
2	2	1	1	1	2	2	1	1	1	1	1
1	1	1	1	1	1	1	1	1	1	2	1
2	2	1	1	1	1	1	1	1	1	1	1
2	2	1	1	1	1	2	2	1	2	1	1
2	2	1	1	1	2	2	2	1	2	1	1
2	2	1	1	2	1	1	1	2	1	1	1

39' 106'

253° 254°

a) 5'x5' Mean Values

2	1
1	1

b) 30′ x 30′ Mean Values

1

c) 1° x 1° Mean Value

Table 10. TC in 5', 30' and 1° Mean Block Values (5' Mean Elevation Data)

Comparing Table 9 with Table 5, we find that if we use the 5'x5' mean elevation data, the mean block values of g_1 will be smoother and the magnitude becomes smaller. For the terrain correction we have the similar conclusion (cf. Table 10 and Table 6). Since the terrain correction depends on the roughness of the topography, the results of the terrain correction are sensitive to the smoothing effects (using the mean block values is a smoothing in the data).

In the following, we want to see what the results will be if we interpolate the data to small grid intervals. We will use the 5'x5' mean elevations and consider this data as point values located at the center of the blocks. Then we interpolate the elevation on to a 1'x1' grid by using a bicubic spline function. The results are given in Tables 11, 12, 13 and 14.

37'

9	19	- 4	- 2	-11	20	34	28	-14	-12	13	41
-10	- 8	- 4	18	26	5	15	43	- 8	-12	- 7	16
10	- 3	- 9	-11	-14	-10	16	40	- 9	-11	-10	12
8	15	20	17	1	14	32	48	7	-12	-10	- 3
- 2	1	10	24	28	26	23	27	49	- 9	- 9	-10
- 1	- 5	- 7	- 9	- 7	31	27	5	53	35	- 6	-10
- 2	- 5	- 4	7	13	30	- 1	7	23	36	24	- 9
- 1	- 3	0	13	29	23	16	- 1	9	11	27	- 7
- 1	2	0	11	25	- 3	13	2	20	11	29	- 9
- 1	- 1	- 5	- 1	6	6	- 5	- 9	9	7	19	1
- 1	- 2	- 3	4	2	11	- 7	- 6	9	13	11	8
- 1	- 1	- 2	- 3	8	3	- 5	25	13	4	1	13

36' 106'

241° 242°

a) 5' x 5' Mean Values

5	11
4	8

b) 30′ x 30′ Mean Values

7

c) 1° x 1° Mean Value

Table 11. g_1 in 5'x5', 30'x30' and 1°x1° Mean Block Values (5'x5'Mean Elevation Data; Interpolated to a 1'x1' Elevation Grid)

37°

10	22	- 5	- 3	-14	23	34	30	-16	-12	12	45
-11	- 9	- 5	19	30	3	14	46	-10	-12	- 8	17
12	- 4	-10	-13	-16	-11	15	43	-12	-11	-11	13
8	16	21	17	- 1	14	33	51	4	-12	-10	- 6
- 3	0	10	25	32	26	22	26	54	-13	- 9	-10
- 1	- 5	- 7	- 9	-10	33	30	2	56	37	- 8	- 9
- 2	- 5	- 5	0	12	32	- 4	9	23	37	26	-10
- 1	- 3	0	13	31	24	17	- 2	10	10	29	- 8
- 2	- 3	0	11	28	- 5	15	2	22	10	32	-11
- 1	- 1	- 5	- 2	5	7	- 6	-10	10	6	20	- 2
- 1	- 2	- 4	5	2	12	- 7	- 7	9	14	12	8
- 1	- 1	- 2	- 3	9	3	- 6	28	13	4	1	14

36° 241° 242° 106°

a) 5'x 5' Mean Values

5	12
4	9

b) 30'x 30' Mean Values

8

c) 1°x 1° Mean Value

Table 12. g_1 in 5'x5', 30'x30' and 1°x1° Mean Block Values (5'x5' Mean Elevation Data; no Interpolation)

37°

5	5	4	3	4	5	7	10	9	6	6	8
5	4	4	4	5	4	5	10	9	6	5	5
4	4	4	4	5	5	6	9	10	8	5	3
5	5	5	5	5	5	6	9	10	8	5	5
4	5	6	6	6	7	6	5	10	11	8	5
4	5	6	6	6	7	6	5	10	11	8	5
3	5	6	6	6	6	4	4	6	8	9	6
3	4	5	7	7	5	4	3	3	4	8	6
3	4	5	7	6	4	4	3	4	4	7	6
3	3	5	5	4	3	3	3	3	3	4	4
2	3	5	4	3	3	2	3	3	3	3	4
2	3	3	4	3	2	3	5	3	2	2	3

36° 241° 242° 106°

a) 5'x5' Mean Values

5	7
4	4

b) 30'x 30' Mean Values

5

c) 1°x 1° Mean Value

Table 13. TC in 5'x5', 30'x30' and 1°x1° Mean Block Values (5'x5' Mean Elevation Data; Interpolated in 1'x1' Mean Elevation)

37°

5	6	4	3	4	5	7	10	9	6	5	9
6	5	4	5	6	4	5	11	8	6	5	5
4	3	4	4	5	4	5	10	9	7	5	4
5	5	6	7	7	6	5	6	13	10	6	5
4	5	6	7	7	6	5	6	13	10	6	5
4	5	6	6	6	7	6	5	11	11	8	5
3	6	5	5	6	7	4	4	6	8	9	7
3	4	5	6	7	6	4	3	4	4	8	6
3	4	5	6	7	4	4	3	4	3	8	6
3	3	6	5	4	3	3	3	3	3	5	4
2	3	5	4	3	3	3	3	3	3	3	3
2	3	3	4	3	2	3	5	3	2	2	4

36° 241° 106° 242°

a) 5'x5' Mean Values

5	7
4	4

b) 30′× 30′ Mean Values

5

c) 1°× 1° Mean Value

Table 14. TC in 5'x5', 30'x30' and 1°x1° Mean Block Values (5'x5' Mean Elevation Data; no Interpolation)

Tables 11-14 show that there are no significant improvements in the results by using interpolation of the elevation to dense point values. From the computing process we know: the integration in the innermost zone (5'x5' square) has no significant contributions to g_1 and TC, because we set the integration in the innermost zone zero when there are no interpolations used.

The gradient correction terms for the gravity anomalies were also computed by using the potential coefficient model OSU86F (Rapp and Cruz, 1986). We use the program written by R. H. Rapp for the correction terms of gravity anomalies in the test region and compare the results in Table 15.

Table 15. Comparison of the Gradient Solution, Terrain Correction and the Correction Terms From the Global Gravity Model OSU86F (Unit:mgal)

♦	λ	height	$-h\frac{\partial \Delta g}{\partial h}$	$\frac{1}{2}h^2\frac{\partial^2 \Delta g}{\partial h^2}$	g_1	TC
39.25	253.25	2632	-0.10	-0.04	5	1
39.25	253.75	2707	0.48	0.05	5	1
39.75	253.25	2721	-0.62	-0.08	-3	1
39.75	253.75	2589	1.53	0.04	1	2
35.25	277.25	839	0.27	0.00	3	0
35.25	277.75	441	-0.25	0.00	1	1
35.25	277.25	789	0.68	0.01	2	1
35.25	277.75	848	0.34	0.01	3	0
36.25	241.25	1406	1.11	0.04	4	5
36.25	241.75	2400	4.72	0.39	9	7
36.75	241.25	2252	2.92	0.09	5	4
36.75	241.75	2352	3.61	0.28	12	4

Table 15 shows that the correction terms of the gravity anomalies by using the Gravity Model OSU86F are much smaller than g_1 and TC.

6. Computations of the Terrain Correction and the Gradient Solution on a Global Basis.

The elevation data in 5′x 5′ mean block values are available from the National Geophysical Data Center, Boulder, Colorado. The elevation data has been used for the computation of the g_1 term and the terrain correction on a global basis.

For the computation of the g_1 term, we make the assumption

$$\Delta g = a + bh \quad , b = 2\pi k\rho$$

The parameters a and b have been taken as constants with b equal to 0.11 mgal/meter.

The integration region is taken as 15° in latitutde extent and 30° in longitude. The boundary (or overlap) of the integration is taken by 50km. This satisfies the accuracy for most situations (Noë, 1980). But the boundary is not large enough for the Himalaya Mountains. Figure 3 shows the differences of the g_1 term by using a 50km boundary and a 250km boundary. The maximum difference is 12 mgals. Figure 4 shows the differences of the terrain correction by using a 50km and a 250km boundary. The maximum difference is 6mgals. In a flat area the differences of the g_1 term and the terrain correction by using the different boundaries are smaller than 1mgal (see Fig. 5). Therefore, we have to take larger boundary if the topography is rough and high in the integration region. In the computations we have taken the 250km boundary for the mountain areas and a 50km boundary for the flat areas.

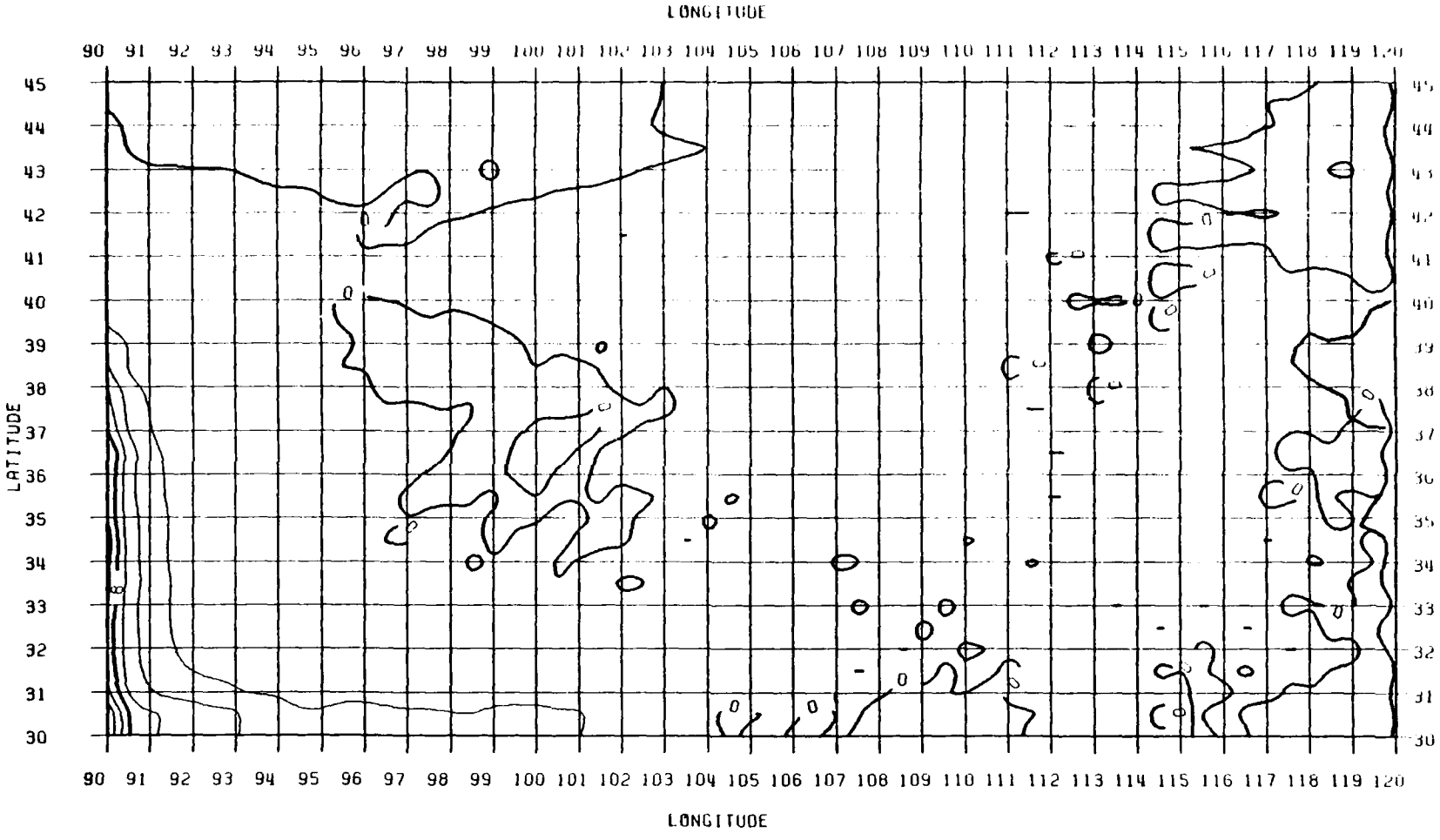

Figure 3. Differences of the g_1 Term Using 50 km and 250 km Boundaries in an Area Containing the Himalaya Mountains; (Contour Interval: 2 mgal)

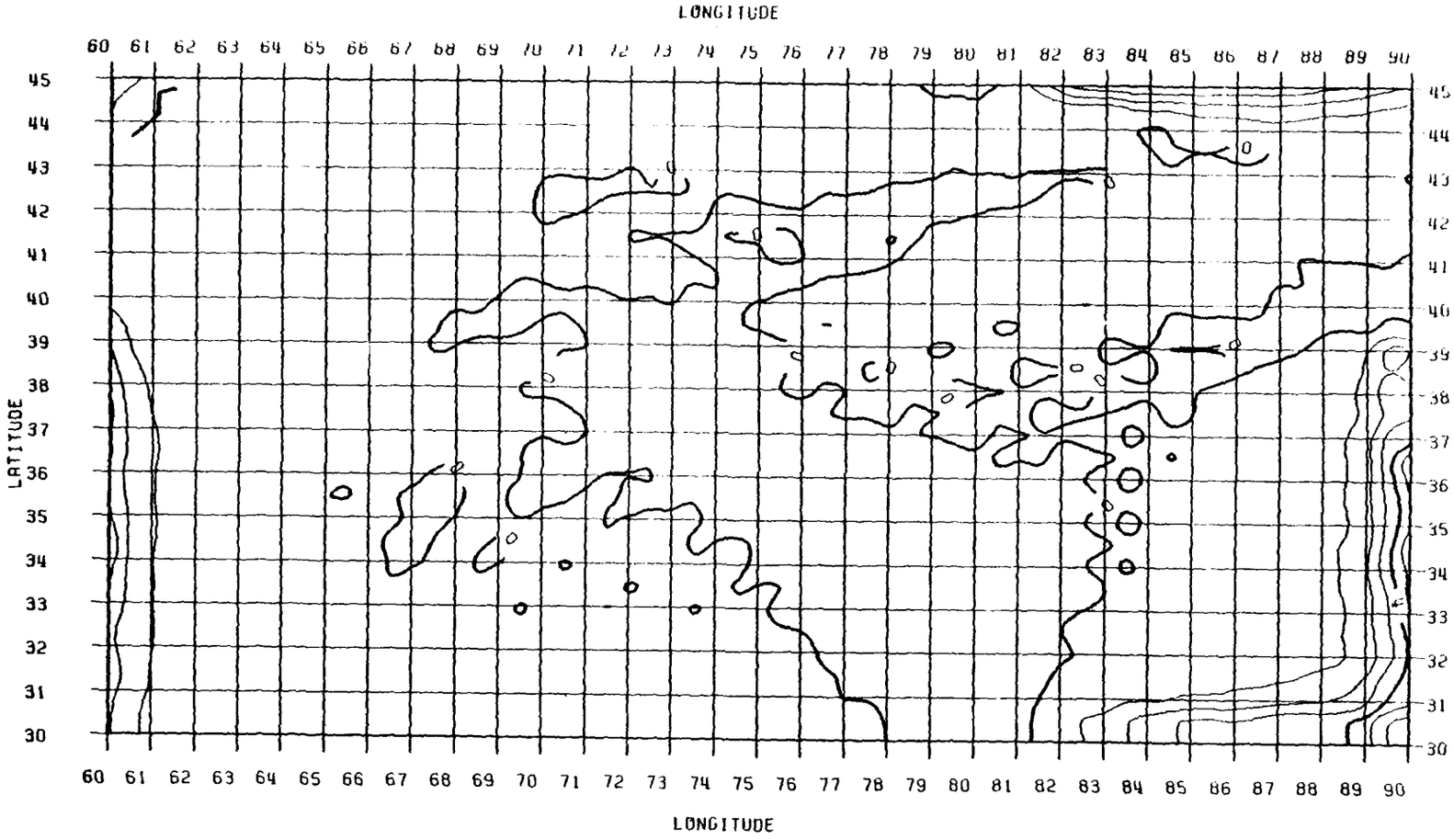

Figure 4. Differences of the Terrain Correction Using 50 km and 250 km Boundaries in an Area Containing the Himalaya Mountains; (Contour Interval: 1 mgal)

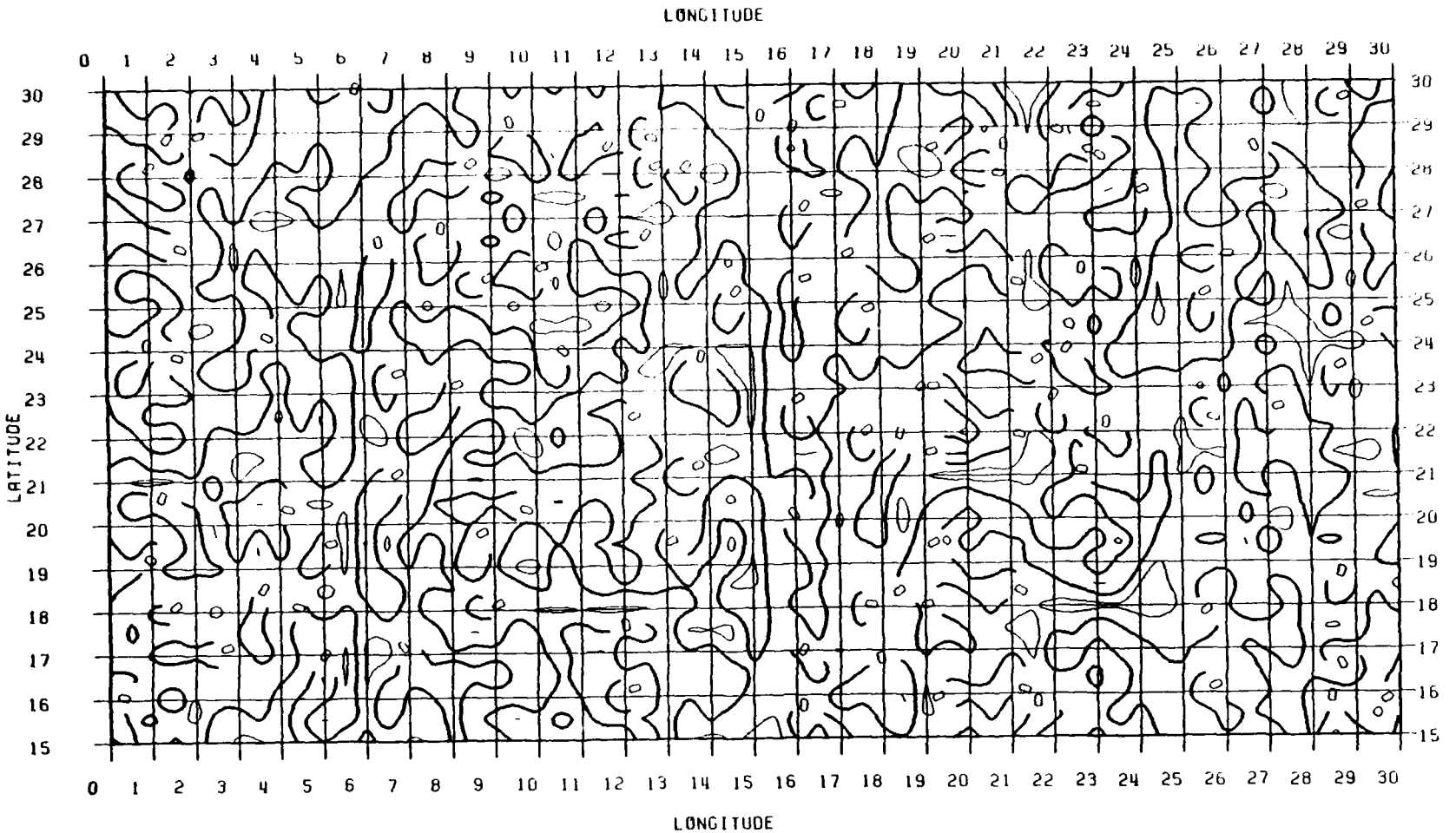

Figure 5. Differences of the g_1 Term due to the Use of 50 km and 250 km Boundaries in a Topographically Flat Area; (Contour Interval: 0.4 mgal)

The g_1 term and the terrain correction are computed in 5' mean block values by using the FFT technique. All computations are completed at the Instruction and Research Compututer Center at The Ohio State University. The CPU time required was about 10^{-3} second for each point on the IBM 3081 at OSU.

Tables 16 and 17 show the distributions of the g_1 term in 5' and 30' mean block values according to the magnitude. g_1 are almost concentrated in the interval [-5,5]. There are only a few larger values for the g_1 term.

Table 16. The Distribution of the g_1 Term According to the Magnitude (5' Mean Block Values)

Interval (mgals)			Numbers	Percentage
-85.	.....	-75.	4	0.000 %
-75.	.....	-65.	24	0.000
-65.	.....	-55.	36	0.000
-55.	.....	-45.	86	0.001
-45.	.....	-35.	274	0.003
-35.	.....	-25.	870	0.009
-25.	.....	-15.	3771	0.040
-15.	.....	- 5.	38846	0.416
- 5.	.....	5.	9123185	97.771
5.	.....	15.	121068	1.297
15.	.....	25.	25428	0.273
25.	.....	35.	7173	0.077
35.	.....	45.	2939	0.031
45.	.....	55.	1391	0.015
55.	.....	65.	5083	0.054
65.	.....	75.	410	0.004
75.	.....	85.	217	0.002
85.	.....	95.	116	0.001
95.	.....	105.	77	0.000
105.	.....	115.	51	0.000
115.	.....	125.	48	0.000
125.	.....	135.	29	0.000
135.	.....	145.	22	0.000
145.	.....	155.	16	0.000
155.	.....	165.	5	0.000
165.	.....	175.	10	0.000
175.	.....	185.	9	0.000
185.	.....	195.	3	0.000
195.	.....	205.	3	0.000
205.	.....	215.	1	0.000
215.	.....	225.	0	0.000
225.	.....	235.	0	0.000
235.	.....	245.	1	0.000

Table 17. The Distribution of the g_1 term According to the Magnitude (30′ Mean Block Values)

Interval (mgals)			Numbers	Percentage
-15.	.....	- 5.	86	0.033 %
- 5.	.....	5.	255893	98.724
5.	.....	15.	2198	0.848
15.	.....	25.	969	0.374
25.	.....	35.	49	0.018
35.	.....	45.	4	0.002
45.	.....	55.	1	0.040

The terrain corrections are concentrated between 0 and 10 mgals. The distribution of the terrain correction according to the magnitude is shown in Tables 18, 19.

Table 18. The Distribution of the Terrain Correction According to the Magnitude
(5′ Mean Block Values)

Interval (mgals)			Numbers	Percentage
0.	.....	10.	9320682	99.887 %
10.	.....	20.	5473	0.059
20.	.....	30.	4652	0.050
30.	.....	40.	321	0.003
40.	.....	50.	30	0.000
50.	.....	60.	9	0.000
60.	.....	70.	3	0.000
70.	.....	80.	6	0.000
80.	.....	90.	9	0.000
90.	.....	100.	9	0.000
100.	.....	110.	2	0.000
110.	.....	120.	2	0.000
120.	.....	130.	0	0.000

Table 19. The Distribution of the Terrain Correction According to the Magnitude
(30′ Mean Block Values)

Interval (mgals)			Numbers	Percentage
0.	.....	10.	259140	99.977 %
10.	.....	20.	5473	0.022
20.	.....	30.	4652	0.001

The statistics of the g_1 term and the terrain correction are exhibited in Tables 20 and 21.

Table 20. Statistics of the g_1 Term in 5' and 30' Mean Block Values Unit: mgal

Block Size	Mean Value	Standard Dev.	Max. Value	Min. Value
5'	0.27	±2.56	442.14	-78.88
30'	0.27	±1.54	45.08	-10.47
1°	0.27	±1.24	25.52	-5.16

Table 21. Statistics of the Terrain Correction in 5' and 30' Mean Block Values; Unit: mgal

Block Size	Mean Value	Standard Dev.	Max. Value	Min. Value
5'	0.23	±1.01	183.57	0.0
30'	0.23	±0.82	25.24	0.0
1°	0.23	±0.74	17.77	0.0

The locations of the absolute values of the g_1 term greater than 5 mgals are plotted in Figure 6. The locations of the terrain correction greater than 5 mgals are shown in Figure 7.

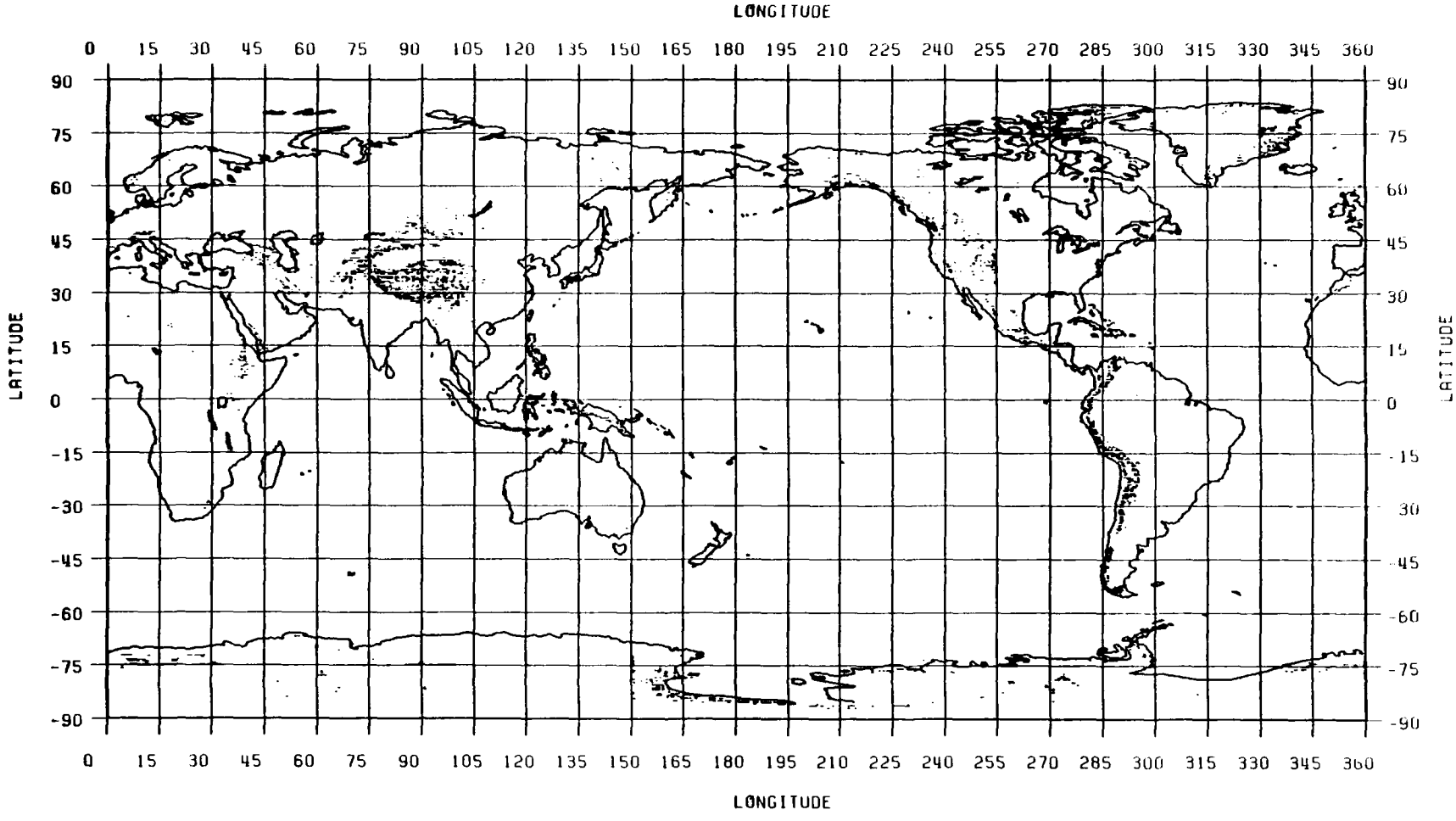

Figure 6. Location of g_1 Values that Exceed 5 mgal in 30′ x 30′ Blocks

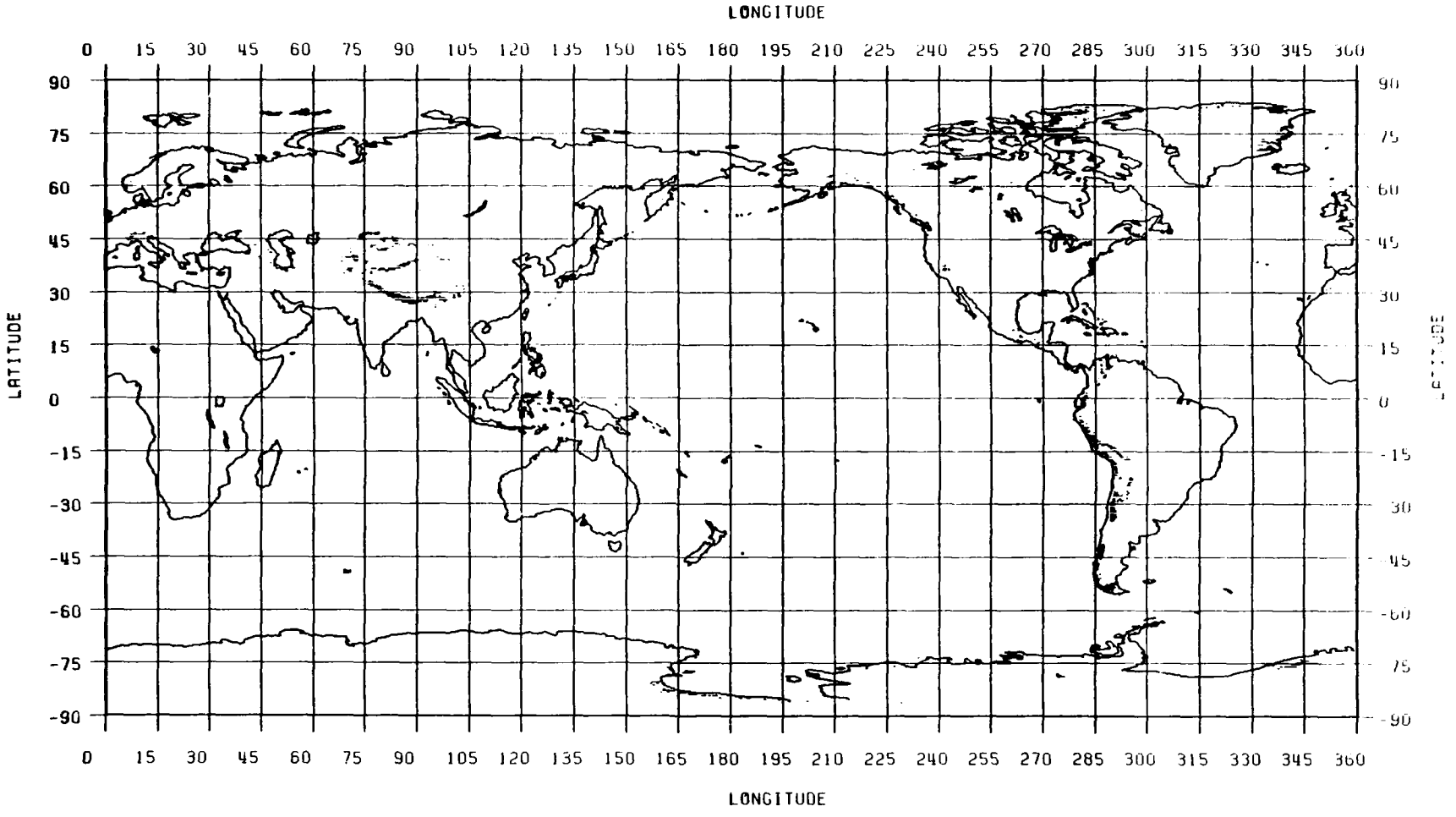

Figure 7. Location of Terrain Correction Values that Exceed 5 mgal in 30′x30′ Blocks

7. Comparison of the Degree Variances of the Gravity Anomaly, the g_1 Term and the Terrain Correction

The corrections of the disturbing potential caused by the g_1 term and the terrain correction can be expanded in spherical harmonics as follows:

$$\delta T^i = \frac{kM}{r} \sum_{n=2}^{N} \sum_{m=0}^{n} \left(\frac{a}{r}\right)^n \left(\bar{C}^i_{nm} \cos m\lambda + \bar{S}^i_{nm} \sin m\lambda\right) \cdot \bar{P}_{nm}(\sin \phi) \qquad i = 1,2 \tag{66}$$

where:

δT^i	correction of the disturbing potential caused by the g_1 term and TC for i = 1, 2, respectively
kM	geocentric gravitational constant
a	equational radius of the reference ellipsoid
$\bar{C}_{nm}$, $\bar{S}_{nm}$	fully normalized potential coefficients
$\bar{P}_{nm}$	fully normalized Legendre function of degree n and order m
r, ϕ, λ	geocentric coordinates

The degree variance of the disturbing potential is defined as (Rapp, 1986, p.10):

$$\sigma_n = \sum_{m=0}^{n} (\bar{C}^2_{nm} + \bar{S}^2_{nm}) \tag{67}$$

For the degree variance, c_n, of the gravity anomaly we have:

$$c_n = \gamma^2 (n-1)^2 \sigma_n \tag{68}$$

where $\gamma = kM/a^2$. In the same manner the degree variances of the corrections to the potential are:

$$\sigma^i_n = \sum_{m=0}^{n} [(\bar{C}^i_{nm})^2 + (\bar{S}^i_{nm})^2] \qquad i = 1,2 \tag{69}$$

and the anomaly degree variances of the g_1 term and TC are

$$c^i_n = \gamma^2 (n-1)^2 \sigma^i_n \qquad i = 1,2 \tag{70}$$

In order to get an impression about the corrections of the g_1 term and the terrain correction on the gravity anomaly the gravity model OSU86E has been used. The percentage of the root mean square (RMS) of the degree variances is defined as following

$$\text{Percentage} = \left(\frac{\sigma n^i}{\sigma n}\right)^{1/2} \cdot 100\% \qquad i = 1,2 \tag{71}$$

The g_1 term and TC in 5' mean block values were used to form $1^\circ \times 1^\circ$

block mean values. The program F419BV3 from Rapp's program library has been used to determine the coefficients of the harmonics spherical of the g_1 term and the TC up to the 180^{th} degree.

The results are drawn in Figure 8. The RMS values of the degree variances of the g_1 term and TC are almost 2 percent of the RMS value of the degree variance of OSU86E. This is smaller than expected.

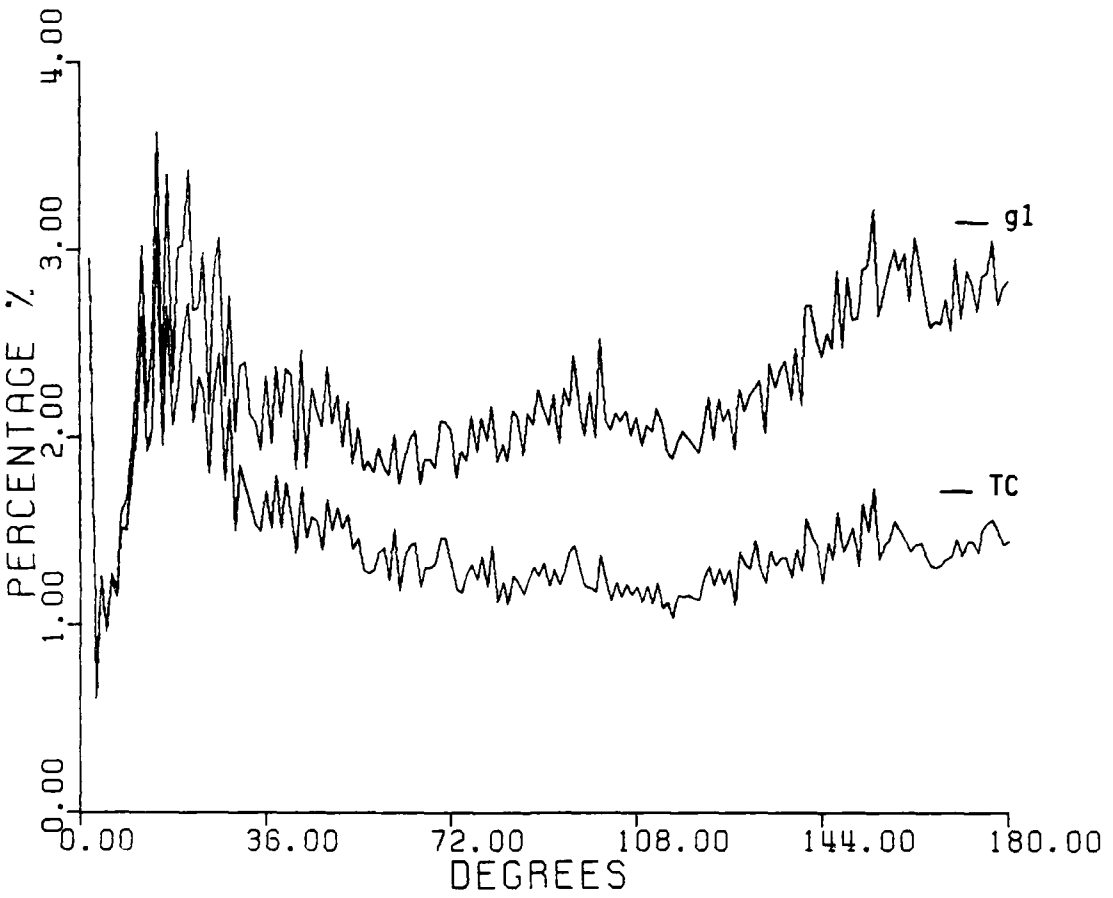

Figure 8. Ratio of the RMS Values of the Degree Variances of the g_1 Term and TC to the Gravity Model OSU86E

The influence of the topography on the gravity anomaly and its spherical harmonic expansion was studied by Rapp (1977). Different models of the terrain correction were used and the correction terms found were on the order of 10 to 30% at the lower degree of the spherical harmonics of the gravity anomaly. The reason for the difference should be due to adopted terrain correction models.

It is very interesting to find that the coefficients of the lower degree of the g_1 term and the terrain correction are almost the same. Figure 9 shows the ratio of the RMS of variances of the g_1 term to TC.

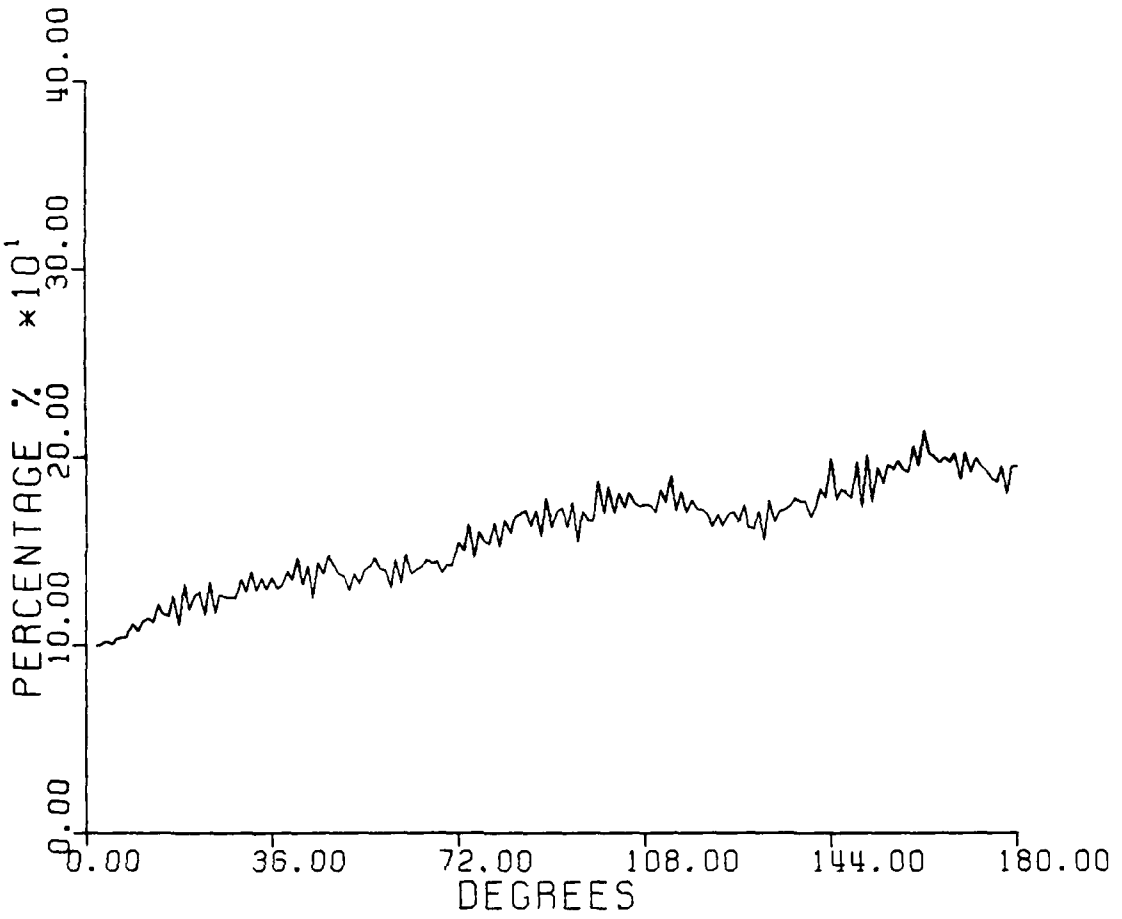

Figure 9. Ratio of the RMS Value of the Degree Variance of the g_1 Term to the RMS Value of the Degree Variance of TC

Theoretically, from (12) we can see that the g_1 term equals the terrain correction plus the integral

$$-\frac{1}{2} K\rho R^2 \iint_{\sigma} \frac{h^2 - h_p^2}{\ell_0^3} d\sigma \qquad (72)$$

The computation shows this integral has no significant contribution on the lower degree of the coefficients of the spherical harmonics of the g_1 term.

8. The Influence of the g_1 Term and TC on the Geoid Undulation and the Deflections of the Vertical

Now we want to know the influences of the g_1 term and TC on the geoid undulation and the deflections of the vertical.

The corrections of the geoid undulation due to g_1 term and TC are

$$\delta N^i = \frac{\delta T^i}{\gamma} \qquad i = 1,2 \quad . \qquad (73)$$

Using (66) and (73) we have the mean square of the corrections of the geoid undulation due to the g_1 term and TC

$$\overline{(\delta N^i)^2} = M\{(\delta N^i)^2\} = a^2 \sum_{n=0}^{N} \sigma_n^i \qquad i = 1,2 \ , \tag{74}$$

where M { } denotes the average over the whole earth. Its definition is given in (Heiskanen and Moritz, 1967, p.252). The RMS of the corrections of the geoid undulation is

$$\sqrt{\overline{(\delta N^i)^2}} = a \sqrt{\sum_{n=0}^{N} \sigma_n^i} \qquad i = 1,2 \tag{75}$$

The values of equation (75) have been evaluated for the g_1 expansion and the terrain correction expansion. These values, for selected degrees, are given in Table 22.

Table 22. RMS Value of the Correction Terms to the Geoid Undulations; Unit: meter

Degree	g_1 term	Terrain Correction
2	0.54	0.54
4	0.13	0.13
5	0.07	0.07
10	0.04	0.04
15	0.02	0.02
20	0.01	0.01
30	0.01	0.01
36	0.01	0.01
50	0.00	0.00
100	0.00	0.00
150	0.00	0.00
180	0.00	0.00

We have two conclusions from the Table 22: the contributions of the g_1 term and the terrain correction to the geoid undulation are the same; only the lower degrees of the spherical harmonic expansions of the correction terms have significant effect on the geoid undulation. The effect of the high degrees (ℓ>36) harmonics of the correction terms are smaller than 1 cm.

The corrections of the deflections of the vertical due to the g_1 term and TC are

$$\underline{\delta\theta^i} = -\frac{1}{a} \operatorname{grad} \delta N^i \tag{76}$$

where $\underline{\theta}$ is the vector of the deflections of the vertical; it has two components, ξ, η.

Using the orthogonal property of the spherical harmonics (Heiskanen and Moritz, 1967, p.262) we have

$$\overline{(\delta\theta^i)^2} = M\{(\delta\theta^i)^2\} = \sum_{n=0}^{N} n\,(n+1)\,\sigma_n^i \qquad i = 1,2 \qquad (77)$$

with

$$(\delta\theta^i)^2 = (\delta\xi^i)^2 + (\delta\eta^i)^2$$

The RMS value of the correction to the deflections of the vertical is

$$\sqrt{\overline{(\delta\theta^i)^2}} = \sqrt{\sum_{n=0}^{N} n(n+1)\,\sigma_n^i} \qquad i = 1,2 \qquad (78)$$

Table 23 shows the RMS value of the corrections of the geoid undulation and the deflections of the vertical. They are in the order 1 meter and 0.1". Here we must recognize that the corrections are mean values the whole earth which are 70% covered by water on which the g_1 term and TC are zero.

Table 23. RMS Value of the Correction of the Geoid Undulation and the Deflections of the Vertical Due to the g_1 Term and TC
Unit: δN in meter; $\delta\theta$ in second

correction	RMS of δN	RMS of $\delta\theta$
g_1	0.7071	0.1129
TC	0.7065	0.0880

9. Conclusion

In order to determine the coefficients of the spherical harmonic expansion of the disturbing potential of the earth in a more precise manner the gravity anomalies have to be analytically downward continued to a simple surface — the chosen ellipsoid. The basic formulas for the downward continuation are the Poisson's integral and the gradient solution (the g_1 term) which is an approximation of the Poisson's integral. The terrain correction has been considered as an approximate method to eliminate the effect of the topography above the ellipsoid.

Because we have no dense gravity anomaly data on a global basis, we approximate the gravity anomaly by using the assumption (10). The elevation in 5' mean block values has been used to compute the g_1 term and the terrain correction on a global basis. Before we started the work, some preliminary tests were done. The digital elevation model in 30'' interval in the United States has been used for the tests. The comparisons of the results which use 30'' point elevation and the elevation in 5' mean block values have been made. The results show that the computation using the elevation in 5'x 5' mean block values are acceptable.

After the computations of the g_1 term and TC in 5' mean block values in a global basis, g_1 and TC are expanded in the spherical harmonics. The influences of the corrections (g_1 and TC) on the disturbing potential of the earth have been studied. The corrections have the order of about 2% of the RMS value of degree variances of the disturbing potential. It is much smaller than expected, especially at the lower degree of the spherical harmonic of the

disturbing potential. The influences of the g_1 term and TC on the geoid undulation (when estimated from expansions of surface gravity data only) have been considered. It takes the order of 1 meter (RMS of correction of the geoid undulation). For the deflections of the vertical the RMS of the corrections of the g_1 term and TC is on the order 0.1".

There are two main error sources in the computations: the assumption (10) and the use of the 5' mean block values. They both are due to lack of the denser gravity anomalies and denser elevation data on a global basis. If the denser data sets are available, then the downward continuation of the gravity anomaly to the ellipsoid can be done more precisely. We can then hope to get a more accurate downward continuation solution needed for the spherical harmonic expansion of the disturbing potential of the earth.

REFERENCES

Bjerhammar, A., A New Theory of Gravimetric Geodesy, Trans. Royal Institute of Technology, Stockholm, No. 243, 1964.

Bracewll, R., The Fourier Transformation and its Applications, McGraw-Hill, New York, 1965.

Euler, H.J., Groten, E., Hausch, W. and Kling, Th., New Results Obtained for Detailed Geoid Approximations, Bolletino di Geodesia e Scienze Affini, Vol., No. 4, 1986.

Forsberg, R., A Study of Terrain Reductions, Density Anomalies and Geophysical Inversion Methods in Gravity Field Modeling, Report No. 355, Dept. of Geodetic Science and Surveying, The Ohio State University, Columbus, AFGL-TR-84-0174; ADA150788, 1984.

Heiskanen, W., and H. Moritz, Physical Geodesy, W.H. Freeman and CO. San Francisco, 1967.

Jekeli, C., The Downward Continuation to the Earth's Surface of Truncated Spherical and Ellipsoidal Harmonic Series of the Gravity and Height Anomalies, Report No. 323, Dept. of Geodetic Science and Surveying, The Ohio State University, Columbus, AFGL-TR-81-0361; ADA112237, 1981.

Pellinen, L.P., A Method for Expanding the Gravity Potential of the Earth in Spherical Harmonics, Translated From Russian, ATIC-TC-1282, NTIS: AD-661819, Moscow, 1966.

Moritz, H., Linear Solutions of the Geodetic Boundary-Value Problem, Report No. 79, Dept. of Geodetic Science and Surveying, The Ohio State University, Columbus, AFCRL-67-0044, AD 653193, 1966.

Moritz, H., Advanced Physical Geodesy, Herbert Wichmann Verlag, Karlsruhe, Abacus Press, Tunbrige Wells, Kent, 1980.

Noë, H., Numerical Investigations on the problem of Molodensity, Mitteilungen der Geodatischen Institute der Technischen Universtät Graz, Folge 36, 1980.

Rapp, R.H., Effect of Certain Anomaly Correction Term on Potential Coefficients Determinations of the Earth's Gravitational Field, Bulletin Geodesique, No. 115, 1975.

Rapp, R.H., Determination of Potential Coefficsients to Degree 52 from 5 Degree Mean Gravity Anomalies, Bulletin Geodesique, No. 1, 1977.

Rapp, R.H., The Relationship Between Mean Anomaly Block Sizes and Spherical Harmonic Representations, Journal of Geophysical Research, Vol. 82, No. 33, 1977.

Rapp, R.H., The Determination of High Degree Potential Coefficient Expansions From the Combination of Satellite and Terrestrial Gravity

Information, Report, No. 361, Dept. of Geodetic Science and Surveying, The Ohio State University, Columbus, 1984.

Rapp, R.H. and J.Y. Cruz, Spherical Harmonic Expansions of the Earth's Gravitational Potential to Degree 360 Using 30' Mean Anomalies, Report No. 376, Dept. of Geodetic Science and Surveying, The Ohio State University, Columbus, 1986.

Sideris, M.G., A Fast Fourier Transform Method for Computing Terrain Corrections, manuscripta geodaetica, Vol. 10, No. 1, 1985.

Sideris, M.G., Spectral Methods for the Numerical Solution of Molodensky's Problem, Ph.D. Dissertation, Department of Surveying Engineering, University of Calgary, 1987.